MECSOL 2022 - Proceedings of the 8th International Symposium on Solid Mechanics
M.L. Bittencourt, J. Labaki, L.C.M. Vieira Jr. and E. Mesquita (Editors), Campinas SP, Brazil, October 17th to 19th, 2022

# Towards a mechanical response of non-aligned graphene layers by the atomic scale finite element method

**Otávio Tovo [1], Daniela Andrade Damasceno [2], Euclides Mesquita [1]**

[1] School of Mechanical Engineering, University of Campinas, 200 Mendeleyev Street, 13083-860, Campinas-SP, Brazil.

[2] Institute of Physics, University of São Paulo, 1371 Matão Street, 05508-090, São Paulo-SP, Brazil.

*Abstract*: A version of the Atomistic Finite Element Method (AFEM) is used to investigate the mechanical properties of bilayer graphene. The AFEM is formulated using the AIREBO potential, which is one of the best existing potentials to simulate hydrocarbons systems such as bilayer graphene, since it considers both covalent and non-bonded interactions. It has recently been reported in the literature that a misalignment of a given angle between the graphene layers has enormous influence on its optical and electrical properties. These properties may change considerably according to the angle of misalignment. But the influence of the angle in the plane relative rotation between the two graphene layers on the mechanical properties of the nano structure has not yet been completely studied. In this article, using the AFEM, equivalent stress-strain curves of a graphene bilayer will be obtained as a function of the misalignment angle between the layers. The role of vacancies of atoms or nano porous on the mechanical properties will also be numerically investigated.

***Keywords: Atomistic Finite Element Method, bilayer graphene, mechanical properties, nanoporous graphene.***

## INTRODUCTION

The mechanical behavior of nanostructures can be investigated by Ab-initio methods (Dirac, 1981), semi-empirical quantum methods (Tadmor and Miller, 2011) and also classical continuum mechanics. Ab-initio methodology presents a better accuracy when compared to semi-empirical quantum techniques, but computationally very expensive. Furthermore, the analyses are still limited to a few hundred or thousand atoms. The molecular dynamics (Alder et al., 1959) represents other alternative to analyze the behavior of nanomaterials.

Liu et al. (2004) claim that the Atomic-Scale Finite Element Method is focused on an energy approach. In other words, this numerical method requires an interatomic energy potential, describing local or non-local bonding forces of an atom interacting with a chosen set of other surrounding atoms. The interatomic energy potentials are formulated based on coordinates of each atom.

The AIREBO potential is one of the most appropriate interatomic energy potentials to simulate hydrocarbon systems since it considers both covalent and non-bonded interactions. Furthermore, it has been successfully employed to design graphene nanostructures and fracture mechanics application (Liu and Chen, 2014). This potential is represented by the sum of three distinct energy potentials: second-generation reactive empirical bond order (REBO) potential energy, Lennard Jones (LJ), and the torsional interactions.

The purpose of this study is to investigate the part of AIREBO potential. Thus, in this paper, it will be addressed the Lennard Jones Potential and Second-Generation Reactive Empirical Bond Order (REBO) Potential Energy. The main idea is joining the three interatomic energy potentials to reach the AIREBO potential.

## STATEMENT OF PROBLEM

This study aims to investigate the mechanical response of non-aligned graphene layers using the atomic scale finite element method. Initially, it is appropriate to consider a simple layer of carbon atoms. This configuration can be seen in Fig. 1. In order to reach the most complete energy potential, it is possible to consider the simple layer to calculate the mechanical response using a single energy potential. The main idea of this paper is to obtain some responses considering a single layer and after that, applying the complete energy potential (AIREBO) to study the mechanical response of bilayer graphene.

According to Fig. 1, it is known that the interaction between layers is represented by Van der Waals bond. This type of bond can be modelled by Lennard Jones Potential. Otherwise, the bond between carbons atoms in the same layer is

represented by covalent bond. This kind of bond can be modelled by second-generation reactive empirical bond order (REBO) potential energy. All these potentials will be discussed in the next sections.

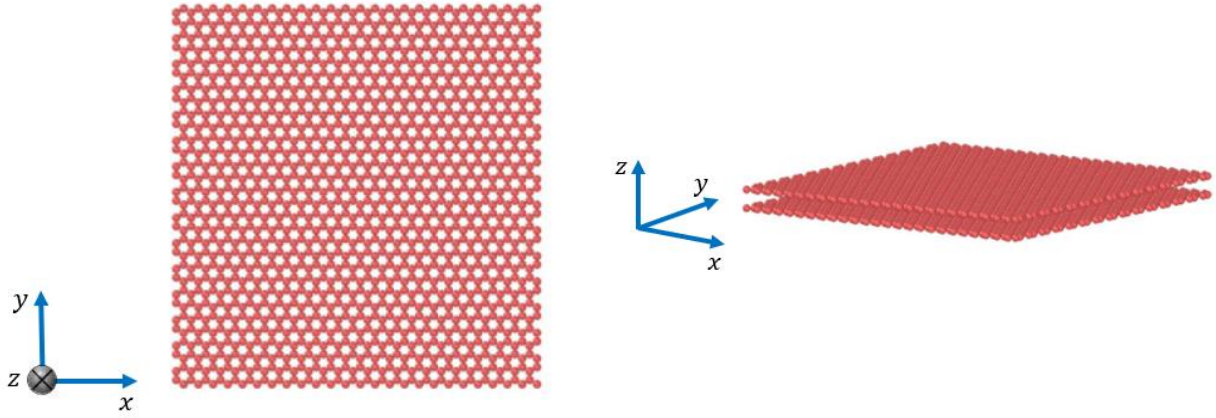


**(a)** **(b)**

**Figure 1 – a) Single layer graphene. b) Bilayer graphene (Mesquita et al., 2021)**

## METHODOLOGY

This section aims to introduce the numerical methods employed in this study. It will be describing a main numerical tool that is able to solve many problems in an atomic scale. Besides that, it will be commented some interatomic energy potentials that provide all the necessary information about the bonding and non-bonding carbon atoms. All the interatomic potentials energy addressed are very important to design the problem about single or bilayer graphene sheet.

### The Atomic-Scale Finite Element Method (AFEM)

Liu et al. (2004) claim that the Atomic-Scale Finite Element Method is focused on an energy approach. In other words, this numerical method requires an interatomic energy potential, describing local or non-local bonding forces of an atom interacting with a chosen set of other surrounding atoms. The interatomic energy potentials are formulated based on coordinates of each atom.

Considering an atomic system with N atoms, the total energy can be expressed by the expression bellow:

$$E_{total} = \sum_{i<j}^{N} E_{ij}\left(x_j - x_i\right) \tag{1}$$

In Eq. (1), the subindexes (i) and (j) correspond to local position of central atom and its surround atoms, respectively.

Basically, the AFEM method applies Eq. (2) to solve the non-linear problem:

$$\mathbf{K}\cdot\mathbf{u} = \mathbf{P} \tag{2}$$

Equation (2) is calculated through an iterative process. The convergence of method is obtained when the norm of force vector (P) reaches a specific tolerance value. In this study, it was adopted the Newton-Raphson method as a tool for the iterative numerical process.

According to Liu et al. (2004), the element stiffness matrix (K) and the non-equilibrium force vector (P) are given by:

$$\mathbf{K}^{element} = \begin{bmatrix} \left(\dfrac{\partial^2 E}{\partial \mathbf{x}_1 \partial \mathbf{x}_1}\right)_{3x3} & \dfrac{1}{2}\cdot\left(\dfrac{\partial^2 E}{\partial \mathbf{x}_1 \partial \mathbf{x}_i}\right)_{3x(3\cdot i-3)} \\ \dfrac{1}{2}\cdot\left(\dfrac{\partial^2 E}{\partial \mathbf{x}_i \partial \mathbf{x}_1}\right)_{(3\cdot i-3)x3} & \left(\mathbf{0}\right)_{(3\cdot i-3)x(3\cdot i-3)} \end{bmatrix}_{(3\cdot i)x(3\cdot i)} \tag{3}$$

$$\mathbf{P}^{element} = \begin{Bmatrix} \left( \mathbf{F}_1 - \dfrac{\partial E}{\partial \mathbf{x}_1} \right)_{3x1} \\ \left( 0 \right)_{(3\cdot i-3)x1} \end{Bmatrix}_{(3\cdot i)x1} \tag{4}$$

In Eq. (3), the term E represents the interatomic energy potential. The subindex (i) indicates the number of atoms in the element type. The element must be carefully chosen according to the energy potential applied. The term F present in Eq. (4) indicates the external force applied to element.

## AIREBO Potential

In this section, a brief approach of the AIREBO potential proposed by Stuart et al. (2000) is introduced.

AIREBO potential is one of the most appropriate interatomic energy potentials to simulate hydrocarbon systems since it considers both covalent and non-bonded interactions. Furthermore, it has been successfully employed to design graphene nanostructures and fracture mechanics application (Liu and Chen, 2014). This potential is represented by the sum of three distinct energy potentials: second-generation reactive empirical bond order (REBO) potential energy, Lennard Jones (LJ), and the torsional interactions. The AIREBO potential can be calculated by the Eq. (5) (Stuart et al., 2000):

$$E^{AIREBO} = \left( \frac{1}{2} \right) \cdot \sum_{i} \sum_{j \neq i} \left[ E_{ij}^{LJ} + E_{ij}^{REBO} + \sum_{k \neq i,\, j} \sum_{l \neq i,\, j,\, k} E_{kijl}^{TORSION} \right] \tag{5}$$

In Eq. (5), the indexes i, j, k and l are related to individual atoms. The term $E_{ij}^{REBO}$ represents the energy stored in bond between atoms i and j (Brenner et al., 2002). The potential $E_{ij}^{LJ}$ considers non-bonded interactions between atoms i and j. Finally, the potential $E_{kijl}^{TORSION}$ includes the energy from torsional interactions between atoms (Liu and Chen, 2014).

## Lennard Jones Potential

In this section, a brief approach of the Lennard-Jones (LJ) potential proposed by Jones (1924) is introduced. It is used to calculate the potential energy of the interaction between two non-bonding atoms based on their bond length ($r_{ij}$):

$$E_{ij}^{LJ} = 4 \cdot \varepsilon \cdot \left[ \left( \frac{\sigma}{r_{ij}} \right)^{12} - \left( \frac{\sigma}{r_{ij}} \right)^{6} \right] \tag{6}$$

In Eq. (6), the parameters σ and ε can describe the intermolecular interactions. The terms σ and ε represent the inter-particle distance and depth of potential, respectively. In this study, these parameters were considered unitary. The term $r_{ij}$ in Eq. (6) means the bond length and can be calculated by:

$$r_{ij} = \sqrt{\left( x_i - x_j \right)^2 + \left( y_i - y_j \right)^2 + \left( z_i - z_j \right)^2} \tag{7}$$

Analyzing Eq. (6), it is possible to verify the influence of two fractions. The first part $(\sigma/r_{ij})^{12}$ represents the strong repulsion, and the second part $(\sigma/r_{ij})^{6}$ describes the attraction force. When the distance between two atoms decreases, the intense repulsion field appears. On the other hand, when the distance increases, the weak attractive field occurs.

The internal force between two elements can be calculated by:

$$F\left( r_{ij} \right) = -\frac{\partial E\left( r_{ij} \right)}{\partial r_{ij}} \tag{8}$$

The first order derivative of energy interatomic potential can be obtained by substituting the Eq. (6) into Eq. (8), yields:

$$F\left( r_{ij} \right) = 4 \cdot \varepsilon \cdot \left[ 12 \cdot \left( \frac{\sigma^{12}}{r_{ij}^{13}} \right) - 6 \cdot \left( \frac{\sigma^{6}}{r_{ij}^{7}} \right) \right] \tag{9}$$

The internal force $F(r_{ij})$ is used to calculate the force vector P in Atomic Scale Finite Element Method.

Other important issue is about the equilibrium distance between two atoms ($r_{eq}$). This parameter can be found by setting the internal force to be zero, yields (Damasceno, 2017):

$$r_{eq} = 2^{\left(\frac{1}{6}\right)} \cdot \sigma = 1.1225 \cdot \sigma \tag{10}$$

When the distance between two atoms represents a value less than $r_{eq}$, the Lennard-Jones field induces a repulsive behavior. In contrast, when the distance is larger than $r_{eq}$ the force has an attractive feature. The maximal force can be found at the intermolecular distance (Damasceno, 2017):

$$r_{F_{\max}} = \frac{1}{\sqrt[6]{\frac{7}{26}}} \cdot \sigma = 1.2445 \cdot \sigma \tag{11}$$

## Second-generation reactive empirical bond order (REBO) potential energy

In this section, a general approach of the second-generation reactive empirical bon order (REBO) proposed by Brenner et al. (2002) is addressed.

The second-generation (REBO) potential energy can be calculated by the Eq. (12) (Brenner et al., 2002):

$$E_{ij}^{REBO} = w_{ij} \cdot \left[ V_{ij}^{R} + b_{ij} \cdot V_{ij}^{A} \right] \tag{12}$$

In Eq. (12), the terms $w_{ij}$ , $V^R$ , $V^A$ and $b_{ij}$ represent the cut-off function, repulsive term, attractive term and bond order term, respectively. These terms are expressed below (Brenner et al., 2002):

$$w_{ij} = \begin{cases} 1, & \left(r_{ij} < D_{\min}\right) \\ \dfrac{\left\{1 + \cos\left[\dfrac{\pi \cdot \left(r_{ij} - D_{\min}\right)}{D_{\max} - D_{\min}}\right]\right\}}{2}, & \left(D_{\min} < r_{ij} < D_{\max}\right) \\ 0, & \left(r_{ij} > D_{\max}\right) \end{cases} \tag{13}$$

In Eq. (13), the terms $D_{min}$ and $D_{max}$ are taken to be 1.7 [Å] and 2.0 [Å], respectively (Brenner et al., 2002).

$$V_{ij}^{R} = \left[1 + \frac{Q}{r_{ij}}\right] \cdot A \cdot e^{\left(-\alpha \cdot r_{ij}\right)} \tag{14}$$

In Eq. (14), the terms Q, A and α are related to type of atom present in the bond.

$$V_{ij}^{A} = -\sum_{n=1}^{3} B^{(n)} \cdot e^{\left[-\beta^{(n)} \cdot r_{ij}\right]} \tag{15}$$

In Eq. (15), the terms $B^{(1)}$, $B^{(2)}$, $B^{(3)}$, $\beta^{(1)}$, $\beta^{(2)}$, $\beta^{(3)}$ are related to type of atom present in the bond. The parameters in Eqs. (14) and (15) can be found in Tab. 1.

$$b_{ij} = \left(\frac{1}{2}\right) \cdot \left[ p_{ij}^{\sigma\pi} + p_{ji}^{\sigma\pi} \right] + \pi^{rc} + \pi^{dh} \tag{16}$$

In Eq. (16), the terms $\pi^{rc}$ is related to number of carbon and hydrogen atoms in the bond. Otherwise, the term $\pi^{dh}$ is related to mesh design. In the example adopted for REBO potential, the mesh configuration is planar, so the parameter $\pi^{dh}$ is set by zero (Brenner et al., 2002).

The terms $p_{ij}^{\sigma\pi}$ and $p_{ij}^{\sigma\pi}$, also present in Eq. (16), are related to the angle between carbon atoms. These terms are calculated by:

$$p_{ij}^{\sigma\pi} = \left[ 1 + \sum_{k \neq i,j} w_{ik} \cdot g\left(\cos\theta_{jik}\right) \cdot e^{\lambda} + P_{ij}\left(N_i^C, N_i^H\right) \right]^{(1/2)} \tag{17}$$

$$p_{ji}^{\sigma\pi} = \left[ 1 + \sum_{k \neq j,i} w_{jk} \cdot g\left(\cos\theta_{ijk}\right) \cdot e^{\lambda} + P_{ji}\left(N_j^C, N_j^H\right) \right]^{(1/2)} \tag{18}$$

The function $g(\cos\Theta_{jik})$ in Eq. (17) is defined for some values for Θ angle between carbon atoms.

Table 1 represents the parameters for the carbon-carbon pair terms. All these values were considered for the second-generation reactive empirical bond order (REBO) potential energy.

**Table 1 – Parameters for the carbon–carbon pair terms (Brenner et al., 2002).**

| Parameter | Value | Unit |
|---|---|---|
| $B^{(1)}$ | 12388.792 | eV |
| $B^{(2)}$ | 17.567065 | eV |
| $B^{(3)}$ | 30.714932 | eV |
| $\beta^{(1)}$ | 4.7204523 | $Å^{-1}$ |
| $\beta^{(2)}$ | 1.4332132 | $Å^{-1}$ |
| $\beta^{(3)}$ | 1.3826913 | $Å^{-1}$ |
| A | 10953.544 | eV |
| Q | 0.313460 | Å |
| α | 4.7465391 | $Å^{-1}$ |

## NUMERICAL RESULTS

This section presents some numerical results from two and three-dimensional domains applying the Atomic-Scale Finite Element Method. In this investigation, it was employed two interatomic energy potentials, the Lennard Jones Potential and Second-generation reactive empirical bond order (REBO) potential energy.

### Lennard Jones Potential 2D

Figure 2a represents a three-dimensional generic system with 22 elements. Initially, the elements are in the equilibrium position. It means that the distance between two elements is set by $r_{eq}$ = 1.1225 [Å] (Damasceno, 2017). According to Fig. 2a, it is possible to identify a force applied to elements 9 and 18, in x direction. For this problem, the force $F_x$ ranges from 0 to 4.0 [eV/Å]. It is important to highlight that some elements (1,5,14,19) are fixed in all directions (x,y,z). Figure 2b illustrate the 3D mesh with one element shifted in z direction.

The strain measure can be obtained through the Eq. (19) bellow:

$$\bar{\varepsilon} = \frac{\sum_{i=1}^{n_{atoms}} \left( \dfrac{L^{(i)} - L_0^{(i)}}{L_0^{(i)}} \right)}{n_{atoms}} \tag{19}$$

In Eq. (19), $n_{atoms}$ indicates the number of tensioned atoms. The parameter $L_0^{(i=1)}$ represents the distance between the atoms 9 and 5 in equilibrium position. The parameter $L^{(i=1)}$, in the same equation, indicates the distance between the atoms 9 and 5 for each step of force, after the convergence. The subindex "i" in parameters L and $L_0$ represents the pair of atoms (tensioned and fixed). In this problem, i=1,2 are related to pairs 9/5 and 18/14 respectively.

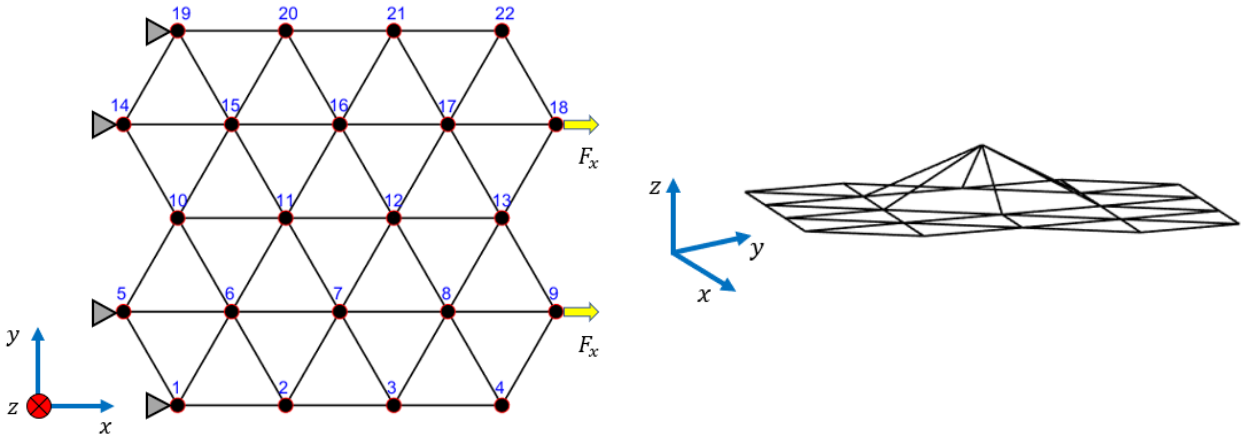


**(a)** **(b)**

**Figure 2 – Hexagonal mesh. a) 2D view. b) 3D view.**

In Fig. 3a the black line indicates the initial mesh (elements in equilibrium position at $F_x = 0$ [eV/Å]), and the red line indicates the deformed mesh at $F_x = 4.0$ [eV/Å]. Figure 3b represents the strain for each step of force obtained by Eq. (19).

Analyzing the results illustrated in Fig. 3b it is possible to infer that 2D and 3D mesh addressed in this study don't present a relevant difference between each other. It means that the shifted element in z direction (Fig. 2b) don't have influence in the mechanical behavior when compared to 2D mesh (all atoms at plain x-y).

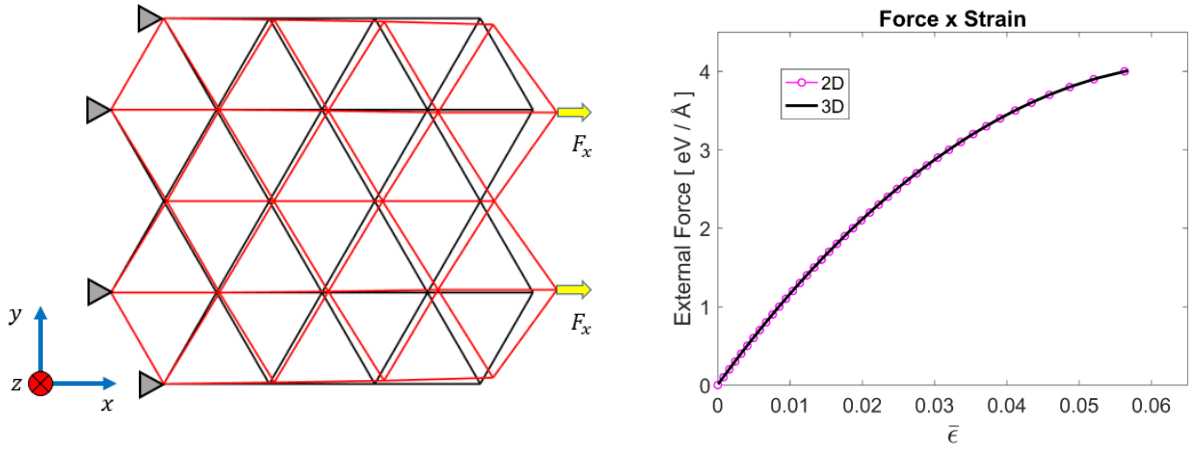


**(a)** **(b)**

**Figure 3 – (a) Hexagonal mesh (equilibrium position and deformed design). (b) Force x Strain.**

## Second-generation reactive empirical bond order (REBO) potential energy

Figure 4a represents a graphene sheet with 28 carbon atoms in armchair direction. Initially, the atoms are in the equilibrium position. It means that the distance between two elements is set by $r_{eq} = 1.396$ [Å] (Brenner et al., 2002). According to Fig. 4a, it is possible to identify a force applied to elements 8,16 and 24, in x direction. For this problem, the force $F_x$ ranges from 0 to 5.2 [eV/Å]. It is important to highlight that some elements (5,13,21) are fixed in all directions (x,y). Figure 4b illustrates a comparison between author's data and Damasceno (2017) about strain for each step of force. According to Fig. 4b, it is possible to verify that the curves are very close each other. This result suggests that the numerical implementation about REBO potential presents an acceptable consistency. The authors believe that this algorithm can be applied to investigate the graphene layers using AIREBO energy potential.

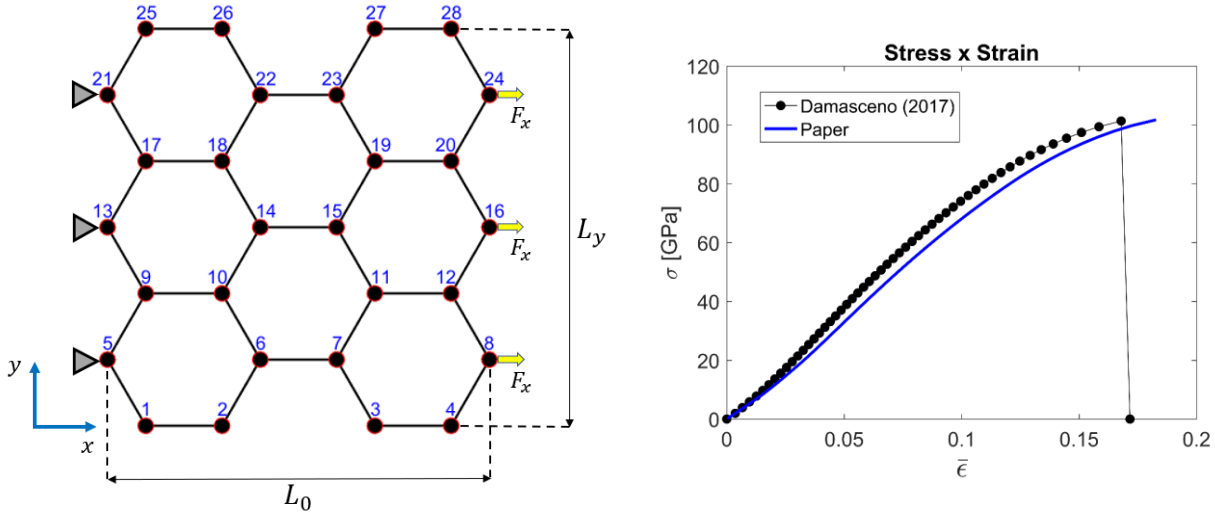


**(a)** **(b)**

**Figure 4 – Graphene sheet with 28 atoms and armchair edges. (a) Atoms in equilibrium position. (b) Stress x Strain.**

The stress value can be approximated by the external load and the area of force application. It is also important to consider all tensioned atoms in the stress value calculation. According to Fig. 4a, the area can be considered by the length ($L_y$) of mesh orthogonal to traction direction, and a specific thickness (t). In this specific problem, the thickness (t) of sheet was assumed as 0.34 [nm], which is the equilibrium distance between two parallel graphene sheets. Thus, the stress for each step force Fx can be calculated by Eq. (20) (Damasceno, 2017):

$$\sigma = \left( \frac{n_{atoms} \cdot F_{ext}}{A} \right) = \left( \frac{n_{atoms} \cdot F_{ext}}{L_y \cdot t} \right) \tag{20}$$

Some parameters of 2D carbon mesh used to calculate area and strain measure can be verified in Fig. 4a. Besides that, Fig. 4b presents the stress-strain curve of pristine graphene sheets obtained from AFEM for uniaxial tensile loading in the armchair direction based on Second-generation reactive empirical bond order (REBO) potential energy.

In order to validate the numerical implementation of REBO potential, it has been considered a graphene sheet with 28 carbon atoms in zigzag direction. Initially, the atoms are in the equilibrium position. It means that the distance between two elements is set by $r_{eq}$ = 1.396 [Å] (Brenner et al., 2002). According to Fig. 5a, it is possible to identify a force applied to elements 25, 26, 27 and 28, in x direction. For this problem, the force $F_x$ ranges from 0 to 5.2 [eV/Å]. It is important to highlight that some elements (1,2,3,4) are fixed in all directions (x,y). Figure 5b illustrates a comparison between author's data and Damasceno (2017) about strain for each step of force. According to Fig. 5b it is possible to verify that the curves are very close each other. Thus, the numerical implementation about REBO potential presents a good agreement.

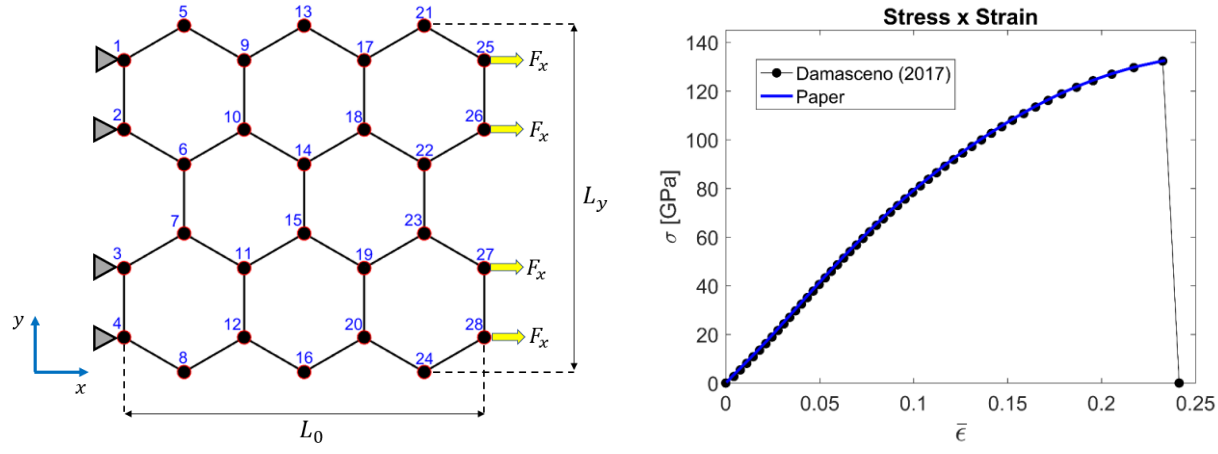


**(a)** **(b)**

**Figure 5 – Graphene sheet with 28 atoms and zigzag edges. (a) Atoms in equilibrium position. (b) Stress x Strain.**

Figure 6a presents a comparison between the strain from pristine graphene sheet in armchair and zigzag direction. According to Fig. 6a, the curves have a similar behavior. Besides that, Fig. 6b presents the stress-strain curve of pristine graphene sheets in armchair and zigzag direction obtained from authors and Damasceno (2017) based on Second-generation reactive empirical bond order (REBO) potential energy. The results suggest that the numerical implementation about REBO potential presents a good agreement. The authors believe the numerical implementations applied in this paper can be employed in investigation of graphene layers using AIREBO energy potential.

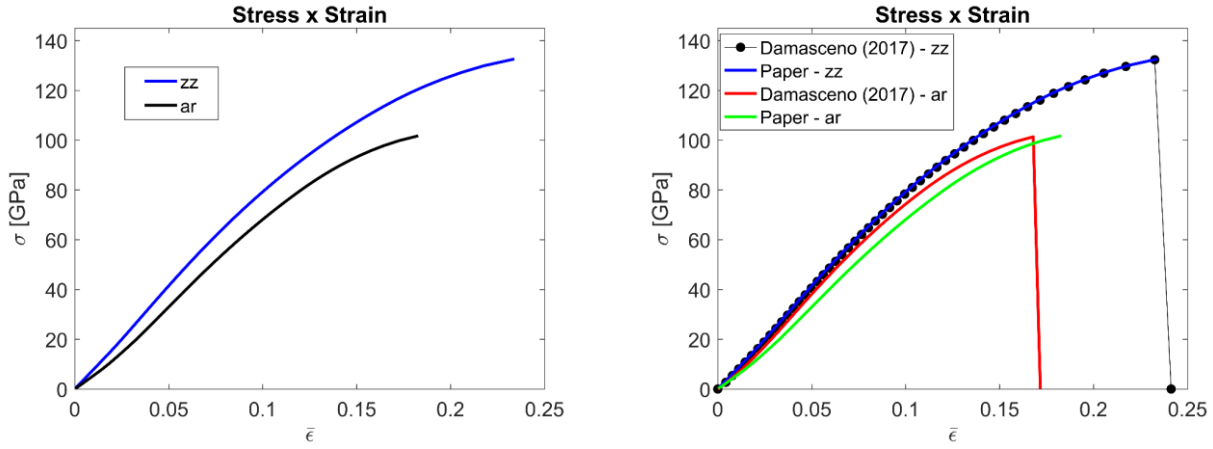


**(a)** **(b)**

**Figure 6 – Stress x Strain. (a) Mesh in armchair (ar) and zigzag (zz) direction. (b) Comparison between authors and Damasceno (2017) data.**

## CONCLUSIONS

This article presented two applications using the Atomic-Scale Finite Element Method (AFEM). The first analysis is based on two and three-dimensional atomic domain governed by the Lennard-Jones interatomic energy potential. The second one corresponds to pristine graphene sheet with armchair and zigzag edges. The graphene sheet, tensioned in armchair and zigzag directions, was investigated through the second-generation reactive empirical bond order (REBO) potential energy.

The results show that the numerical methods and its implementation are consistent. All the situations considered in this study were compared with other researcher's works. It is important to highlight that both interatomic potentials energy employed are totally necessary to study the AIREBO potential, which corresponds to the most appropriate method to investigate the mechanical behavior of bilayers graphene sheet.

The next step is to investigate the Torsion potential energy. It was commented previously that the AIREBO potential represents the sum of three interatomic energy potentials. Thus, when all potentials energy cited (Lennard-Jones, REBO and Torsion) were consistent, it will be possible to apply the AIREBO potential to study completely the bilayers graphene sheet.

## ACKNOWLEDGMENTS

The research leading to this work was funded by the São Paulo Research Foundation (Fapesp) through grant FAPESP CEPID Process 2013/08293-7 and Coordenação de Aperfeiçoamento de Pessoal de Nível Superior - Brasil (CAPES) - Finance Code 001. Damasceno also thanks to the Research Centre for Gas Innovation, SHELL Brazil, and the financial support of FAPESP, grant 2020/01558-9.

## REFERENCES

Alder, B.J., Wainwright, T.E.J., 1959. "Studies in Molecular Dynamics. I. General Method", The Journal of Chemical Physics, Vol. 31, pp. 459-466.

Brenner, D. W., Shenderova, O. A., Harrison, J. A., Stuart, S. J., Ni, B. and Sinnott, S. B., 2002, "A second-generation reactive empirical bond order (REBO) potential energy expression for hydrocarbons", Journal of Physics: Condensed Matter, Vol. 14, No. 4, pp. 783-802.

Damasceno, D.A, 2017, "Nonlinear Atomic-scale Finite Element Method for the Modelling of Nanomaterials and Nanostructures", PhD thesis, University of Campinas, p. 110.

Dirac, P.A.M., 1981, “The Principles of Quantum Mechanics”, Clarendon Press, Oxford.

Jones, J.E., 1924, “On the determination of molecular fields - II. From the equation of state of a gas”, Proceedings of the Royal Society A, Vol. 106, pp. 463–477.

Liu, B., Chen, K.C., 2014, “The atomic-scale finite element method”, Computer Methods in Applied Mechanics and Engineering, Vol. 193, No. 17-20, pp. 1849-1864.

Liu, B., Huang, Y., Jiang, H., Qu, S., Hwang, K.C., 2004, “The atomic-scale finite element method”, Computer Methods in Applied Mechanics and Engineering, Vol. 193, No. 17-20, pp. 1849-1864.

Mesquita, E., Damasceno, D.A., Tovo, O.A., 2021, “Mechanical response of bilayer graphene under different loading modes”, Proceedings of the joint XLII Ibero-Latin-American Congress on Computational Methods in Engineering and III Pan-American Congress on Computational Mechanics, Vol. 1, Rio de Janeiro, Brazil, pp. 41-44.

Stuart, S.J., Tutein, A.B., Harrison, J.A., 2000, “A reactive potential for hydrocarbons with intermolecular interactions”, The Journal of chemical physics, Vol. 112, No. 14, pp. 6472-6486.

Tadmor, E.B., Miller, R.E., 2011, “Modeling materials: continuum, atomistic, and multiscale techniques”, Cambridge University Press, New York.

## RESPONSIBILITY NOTICE

The author(s) is (are) the only party(ies) responsible for the printed material included in this paper.